Universal patterns of equilibrium cluster growth in aqueous sugars observed by dynamic light scattering

D. L. Sidebottom and Tri D. Tran
Department of Physics, Creighton University, Omaha, Nebraska 68178, USA
(Received 14 July 2010; revised manuscript received 28 September 2010; published 3 November 2010)

Dynamic light scattering performed on aqueous solutions of three sugars (glucose, maltose and sucrose) reveal a common pattern of sugar cluster formation with a narrow cluster size distribution. In each case, equilibrium clusters form whose size increases with increasing sugar content in an identical power law manner in advance of a common, critical-like, percolation threshold near 83 wt % sugar. The critical exponent of the power law divergence of the cluster size varies with temperature, increasing with decreasing temperature, due to changes in the strength of the intermolecular hydrogen bond and appears to vanish for temperatures in excess of 90 °C. Detailed analysis of the cluster growth process suggests a two-stage process: an initial cluster phase formed at low volume fractions, ϕ, consisting of noninteracting, monodisperse sugar clusters whose size increases $\phi^{1/3}$ followed by an aggregation stage, active at concentrations above about ϕ=40%, where cluster-cluster contact first occurs.

DOI: 10.1103/PhysRevE.82.051904 PACS number(s): 87.64.Cc, 87.15.−v, 64.60.ah, 78.35.+c

I. INTRODUCTION

Modern cryopreservation of biological tissues requires the infusion of an appropriate solution, known as a cryopreserving agent (CPA), prior to cooling below the freezing point of water [1]. Commericial CPA's contain a variety of additives, some of which are included to maintain proper cellular chemistry and others which are designed to inhibit substantial intracellular ice formation. Among these ingredients are simple sugars (e.g., glucose, sucrose) that are also key to naturally occurring survival processes in many animal species [2,3].

Although sugars are a common component in both synthetic and natural CPA's, the mechanism by which sugar bestows protection to biomatter is not fully understood. Two prominent theories, the vitrification model and the water replacement model, have been proposed [3]. In unprotected tissue, crystallization of the aqueous medium often results in the formation of intracellular ice whose expansion ruptures the cell wall and whose sharp facets can lacerate delicate biological tissues [1]. In the vitrification model [4], it is believed that the incorporation of sugar into water produces a solution that solidifies to a glass as opposed to a crystal. At sufficiently high sugar contents, aqueous sugar solutions are easily vitrified and could thus provide a medium for biotissues that undergoes no catastrophic structural rearrangements during solidification [5]. In the water replacement model [6], it is believed that sugar molecules preferentially bond to biotissue to produce a carbohydrate layer. Water molecules are expelled in this process and, although they may crystallize on cooling, they only produce, nonlethal, extracellular ice.

The propensity for sugar molecules to form intermolecular hydrogen bonds has been demonstrated both by molecular dynamics (MD) simulations [7–11] and recent dynamic light scattering studies [12] of aqueous sugars. In the MD simulations by Lerbret *et al.* [11], the authors observed increasing intermolecular hydrogen bonding for trehalose, maltose, and sucrose solutions with increasing sugar concentration and evidence for the formation of a continuous, hydrogen-bonded carbohydrate network at a percolation threshold of 66 wt % sugar (the limit of their simulations). In our recent study of aqueous glucose solutions using dynamic light scattering [12], we observed the diffusion of glucose clusters in solution as a function of the sugar concentration. We too observed that the cluster size increased with glucose content and appeared to diverge in the vicinity of 80 wt % glucose. In this vicinity of sugar concentrations, an additional viscoelastic relaxation, associated with the slowing structural relaxation of the solution as a whole, was also observed. Even more recently, Kaminski *et al.* [13] observed evidence for cluster formation in molten glucose in the form of an additional dielectric loss feature present at frequencies below that of the main viscoelastic relaxation. The dielectric strength of this additional feature was reasonably constant at low temperatures, but decreased abruptly at elevated temperatures. Together with FTIR measurements of the OH bands, the authors concluded that at temperatures above 366 K the clusters become unstable and likely disintegrate.

Here, we report the results of a companion study conducted on aqueous maltose solutions. Maltose is the dissacharide form of glucose (constructed of two glucose rings) and is a natural extension of our previous investigation. We find much the same dynamics in maltose including both a viscoelastic mode and a diffusional mode associated with the Brownian motion of maltose clusters. However, here we show conclusively the percolation of a hydrogen-bonded carbohydrate network as evidenced by a power law divergence of the mean cluster size as a function of the sugar concentration. Moreover, this power law feature is universal, occurring identically for glucose, maltose, and sucrose solutions. Although the power law growth of the mean cluster size suggests a relation to such phenomena as aggregation, the cluster size distribution is surprisingly monodisperse. Indeed, at low concentrations far from the percolation threshold, cluster formation appears to mimic that of colloidal systems [14–16] in which clusters assume a nearly uniform size due to stabilizing interactions [17]. Based on our findings, we propose that sugar clusters develop in a two stage process

involving first the development of a so-called "cluster phase" [15] consisting of isolated clusters, followed at higher concentrations by a process of cluster-cluster aggregation enroute to percolation of a carbohydrate network.

II. EXPERIMENT

Aqueous solutions of maltose at concentrations below 40 wt % were produced by mixing maltose monohydrate (Fisher) with de-ionized water (Milli-Q) in a beaker over mild heat (ca. 40 °C) until completely dissolved. The solution was then filtered through a 0.05 micron Teflon filter (Millipore) directly into a precleaned scattering cell (25 ml Wheaton vial) to remove undesirable dust particulates. Samples above 40 wt % were similarly produced by first filtering a solution of lower weight percent and slowly evaporating off the water at 60 °C until the desired concentration was achieved by weight analysis.

Details of our dynamic light scattering experiment can be found elsewhere [12]. Light, elastically scattered by the sample, is imaged onto a 50 μm pinhole and allowed to diffract over approximately 50 cm distance where it is recorded by a PMT (Electron Tubes 8963B) operated at a reduced voltage to minimize afterpulsing. Photopulses from the PMT are amplified and discriminated into a corresponding TTL signal whose intensity-intensity autocorrelation function,

$$C(q,t) = \frac{\langle I(0)I(t)\rangle}{\langle I\rangle^2}, \tag{1}$$

is computed by a commercial correlator (Correlator.com). In the current situation of homodyne detection [18], this correlation function is related to the dynamic structure factor, $S(q,t)$, by

$$C(q,t) = 1 + A_{coh}|S(q,t)|^2, \tag{2}$$

where $A_{coh}(=0.73 \pm 0.03)$ is an instrumental constant calibrated using the autocorrelation function obtained from a suspension of monodisperse polystyrene spheres.

Measurements were conducted on samples from 5 to 85 wt % maltose at a fixed scattering angle of 36.9° for temperatures from −10 to 40 °C and at a range of scattering angles for a 65 wt % sample at 13.1 °C. For quasielastic light scattering, the scattering angle defines the scattering wave vector,

$$q = (4\pi n/\lambda)\sin(\theta/2), \tag{3}$$

where n is the index of refraction of the medium. The index of refraction was obtained by a straightforward interpolation of values available in the literature [19].

III. RESULTS

For compositions less than about 75 wt % maltose, we observed a single, exponential decay of the dynamic structure factor. An example is shown in Fig. 1 for the case of 65 wt % maltose whose relaxation time increases with decreasing temperature. The increasing level of scatter in

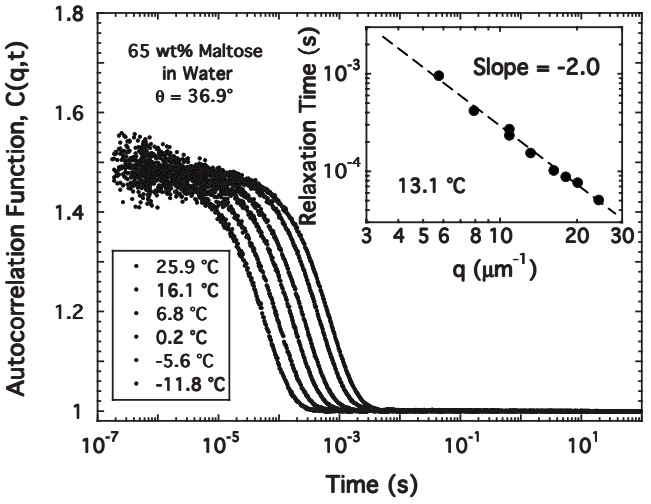

FIG. 1. The intensity-intensity autocorrelation recorded for a 65 wt % solution of maltose at a scattering angle of 36.9°. The spectra are labeled left to right in order of decreasing temperature. Inset shows the relaxation time for the same sample recorded at a fixed temperature of 13.1 °C as a function of the scattering wave vector and illustrates the diffusive character of this relaxation process.

$C(q,t)$ at decreasing times simply results from the limited scattering intensity of our solutions that reduces statistics at short lag times, but has minimal impact on our determination of the decay time occurring at much longer lag times. A study of the angular dependence of this mode was conducted at 13.1 °C and the results, illustrated in the inset to Fig. 1, confirm that the mode is a diffusional process such that [18]

$$S(q, t > 0.1\ \ \mu\text{s}) = Ae^{-t/\tau} = Ae^{-Dq^2t}, \tag{4}$$

where D is the diffusion coefficient.

At higher sugar concentrations, we observe an additional relaxation mode present itself. An example is shown for a 79.8 wt % solution in Fig. 2. At high temperatures, only the diffusional mode discussed previously is present. But, with decreasing temperature, a second relaxation mode is seen to encroach and overtake this diffusional mode. At temperatures where this second mode dominates the entire spectrum, the relaxation is found to be nonexponential and adequately described by

$$S(q, t > 0.1\ \ \mu\text{s}) = A_2 \exp[-(t/\tau_2)^{\beta}], \tag{5}$$

with $\beta = 0.45 \pm 0.05$. A similar, nonexponential relaxation was observed also in glucose solutions and identified as the viscoelastic relaxation of the medium occurring in response to the impending glass transition. To confirm that this new process seen in maltose is the viscoelastic relaxation, we consider how its relaxation time extrapolates with decreasing temperature. Shown in the inset to Fig. 3 is the relaxation time, $\langle\tau_2\rangle = [\Gamma(\beta^{-1})/\beta]\tau_2$, plotted against inverse temperature for a sample at 85 wt % maltose. The data points are seen to extrapolate to the customary glass transition value of $\langle\tau_2\rangle = 100$ s near −14 °C. As illustrated in Fig. 3, this value for the glass transition is in excellent agreement with calorimetric measurements taken from the literature [5].

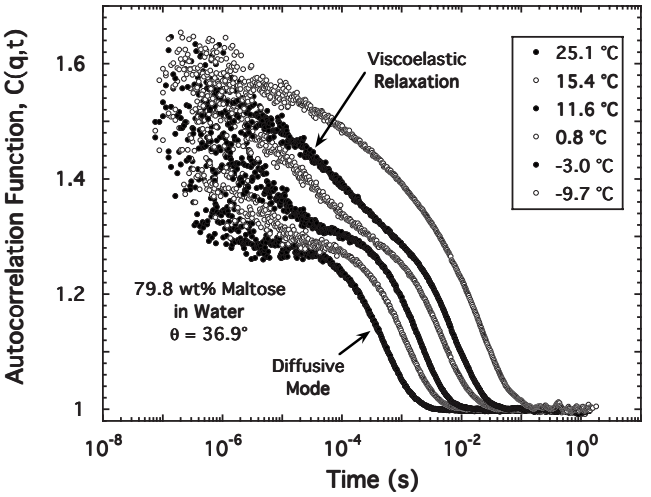

FIG. 2. The intensity-intensity autocorrelation recorded for a 79.8 wt % solution of maltose at a scattering angle of 36.9°. The spectra are labeled left to right in order of decreasing temperature. Evident in the figure is the encroachment of a second, viscoelastic relaxation that fully engulfs the diffusional process at temperatures below −10 °C.

At this point, the findings for maltose are similar to those seen previously for glucose solutions; namely, two relaxation modes (one diffusional and the other viscoelastic) are observed. Due to limitations on our cryostat, we were unable to explore in much detail the viscoelastic mode except at very high sugar concentrations. Instead, we now examine the features of the diffusional process and consider its properties in further detail.

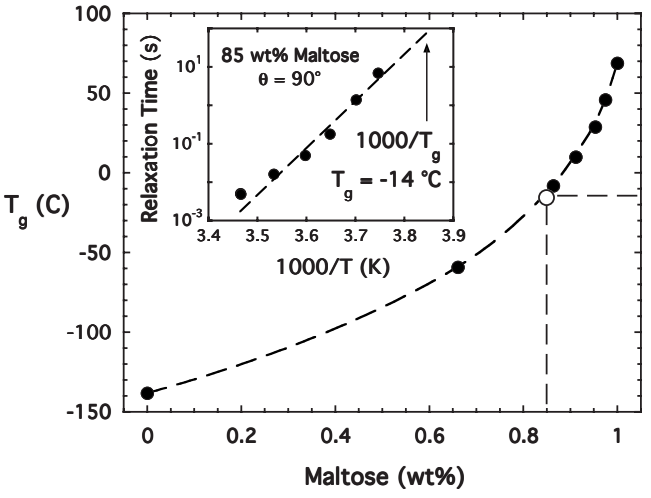

FIG. 3. The glass transition temperature of aqueous maltose obtained by calorimetric methods [5]. The open circle locates the T_g for 85 wt % maltose obtained by dynamic light scattering and confirms the viscoelastic character of the second relaxation. Inset shows the average relaxation time of the viscoelastic relaxation for a 85 wt % solution of maltose. The dashed line is an extrapolation to the apparent glass transition temperature $T_g=-14$ °C where $\langle\tau_2\rangle=100$ seconds.

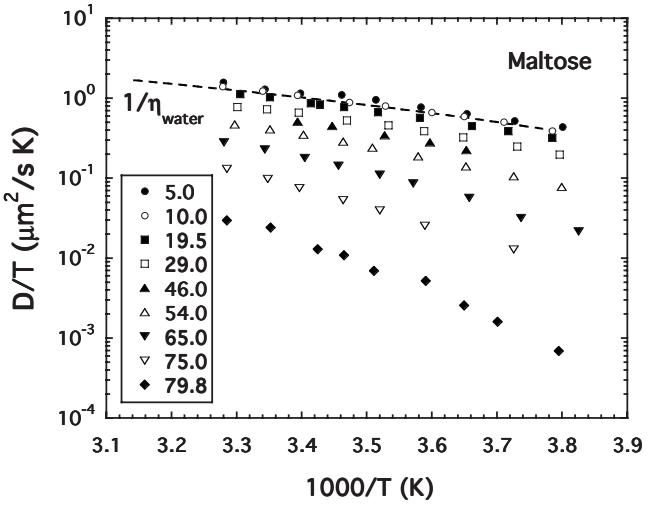

FIG. 4. Temperature dependence of the diffusion coefficient (divided by T) for maltose solutions of various wt % (shown in key). The dashed line indicates the inverse of the viscosity of water (in mPas) over the same temperature range.

IV. ANALYSIS

Diffusional motions in a solution are generally ascribed to Brownian forces and the diffusion coefficient can be described by the Einstein relation,

$$D = kT/\zeta \tag{6}$$

or by the Stokes-Einstein relation for stick boundary conditions,

$$D = \frac{kT}{6\pi\eta_B R_H}, \tag{7}$$

where the drag coefficient, $\zeta=6\pi\eta_B R_H$, depends upon both the viscosity of the Brownian medium (η_B) and the hydrodynamic radius (R_H) of the diffusing object. To begin, we consider the quantity D/T plotted in Fig. 4 for maltose and in Fig. 5 for glucose as a function of the inverse temperature. The value of D is determined from exponential fits of the diffusional mode using Eq. (4) above and, from Eq. (6), the quantity D/T is seen to be proportional to the inverse of the drag coefficient.

In Figs. 4 and 5, we see that the drag coefficient generally increases with increasing sugar content in both cases and that the slope increases considerably at high sugar concentrations. In this sense, the concentration and temperature variations displayed in the figure are similar to the self diffusion coefficients of sucrose and trehalose measured by Rampp *et al.* using NMR techniques [20]. Also included in the figure is the inverse of the viscosity of water [19] (in mPas). The inverse viscosity of water is seen to parallel the quantity D/T at low sugar concentrations (below about 30 wt %) and suggests that, at each composition, objects of a fixed size are diffusing in a Brownian fluid comprised of water. Furthermore, because the quantity D/T decreases in this range of low sugar concentrations, it appears that the size of the diffusing objects is increasing with increasing sugar content.

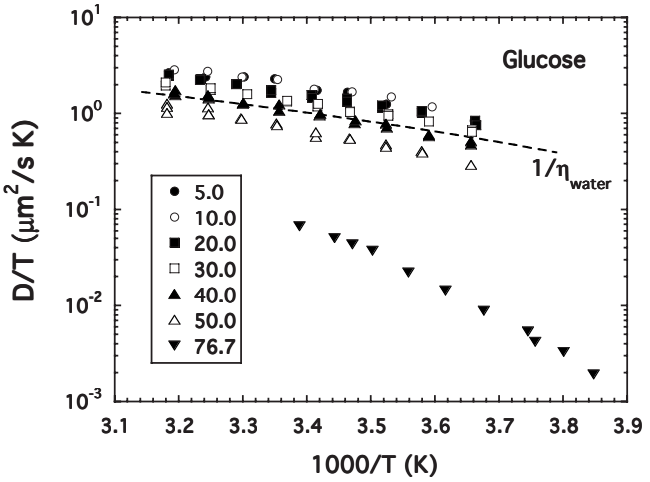

FIG. 5. Temperature dependence of the diffusion coefficient (divided by T) for glucose solutions of various wt % (shown in key). The dashed line indicates the inverse of the viscosity of water (in mPas) over the same temperature range.

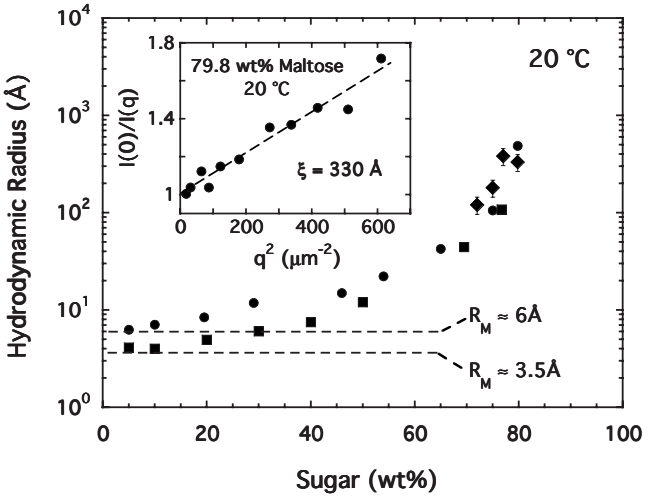

FIG. 6. The hydrodynamic radius of maltose (circles) and glucose (squares) determined at 20 °C using the viscosity of water. The two horizontal dashed lines highlight the approach, in the dilute limit, of the hydrodynamic radius to values consistent with monomeric sugar molecules. Values of the correlation length, ξ, obtained from select maltose solutions by static light scattering (filled diamonds) are also included. Inset illustrates the Ornstein-Zernike analysis of the static light scattering from a 79.8 wt % solution of maltose.

At concentrations above about 30 wt %, the quantity D/T no longer parallels that of the inverse viscosity of water. Here, it is unclear whether the diffusing particles are continuing to increase in size or whether the Brownian medium is thickening beyond that of water or whether both are occurring simultaneously. In an effort to understand the nature of our diffusing objects, we begin in the dilute limit where the Brownian medium is clearly that of water. Using the viscosity of water, we have determined the hydrodynamic radius of the diffusing objects across the entire composition range using the Stokes-Einstein relation in Eq. (7). The results shown in Fig. 6 indicate that, in the limit of vanishing sugar, the hydrodynamic radius is comparable to the size of a sugar molecule, R_M (maltose radius of about 6 Å and roughly twice that of glucose). These are quite small Brownian particles, but appear to be within the realm of validity for the Stokes-Einstein relation according to a recent study [21].

Over the range of concentrations up to about 30 wt %, where use of viscosity of water seems justified, we find that the particle size roughly doubles and suggests the formation of sugar clusters with an average number of monomers, $n_s^c \approx (R_H/R_M)^3 \approx 8$. But what of higher concentrations? The continued use of water as the viscosity of the Brownian fluid becomes questionable, especially in light of its deviation from D/T seen in Figs. 4 and 5, but also because at sufficiently high concentrations one might expect interactions between clusters that violate the intention of the Stokes-Einstein law. Despite this, we choose to continue using water as our Brownian medium in determining the particle size and offer up the following points in way of justification:

(1) Even in a monomeric solution (in which the sugar molecules remain unclustered), the critical concentration at which insufficient water is available to provide proper hydration of the sugar is in the vicinity of 50 wt %. At this concentration there are only 19 water molecules per dissacharide molecule [20]. If clustering were not present, we should anticipate violations of the Stokes-Einstein law to develop near this critical concentration. However, this critical concentration is only relevant for a monomeric solution. Since it is clear that sugar molecules are clustering even below 50 wt %, this clustering inherently generates an *excess* of water beyond that of the requirements for hydration of the sugar. To see this, suppose that a sugar cluster assumes a random closed packed form with a 60% packing efficiency. The number of sugar monomers contained in a cluster is

$$n_s^c \approx 0.6(R_H/R_M)^3, \tag{8}$$

where R_M is the monomer radius. These same sugar molecules in their monomeric form would require $n_w^o \approx n_s^c n_H$ water molecules to participate in hydration, where n_H is the hydration number. However, hydration of the cluster requires a much smaller number of water molecules proportional to the cluster surface

$$n_w^c \approx (R_H/R_M)^2 n_H. \tag{9}$$

Thus, in this simplistic argument, the fraction of excess water,

$$\frac{n_w^{ex}}{n_w^o} = \frac{n_w^o - n_w^c}{n_w^o} = 1 - \frac{n_w^c}{n_w^o} \approx 1 - \frac{R_M}{0.6R_H} \tag{10}$$

actually increases with increasing cluster size thus serving to maintain the water-like Brownian medium for cluster diffusion.

(2) Second, in an effort to assess cluster size in a nondiffusional manner, we have also performed a limited number of studies on maltose solutions using static light scattering techniques. Density fluctuations of a size ξ are known to produce excess scattering in the forward direction described by the Ornstein-Zernike [18] formula

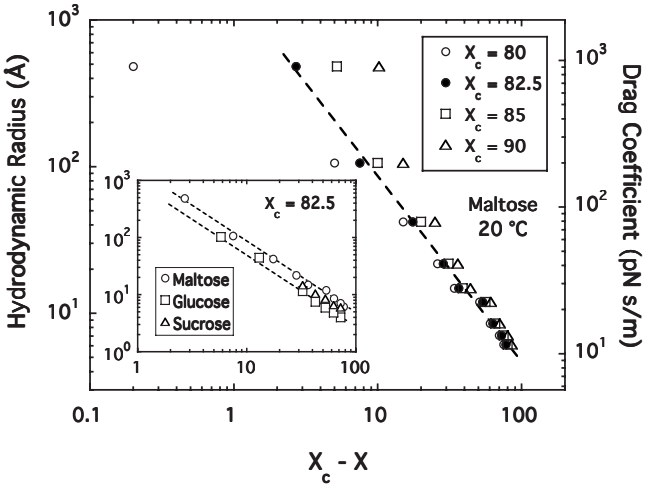

FIG. 7. The hydrodynamic radius of maltose at 20 °C obtained using water as the Brownian medium is plotted against the wt % of maltose relative to four possible choices for a critical wt %, X_c (shown in key). Best overall linearity is found for X_c=82.5 wt % (filled symbols). Inset shows that, for X_c=82.5 wt %, an identical power law divergence of the hydrodynamic radius is seen for maltose, glucose, and sucrose solutions.

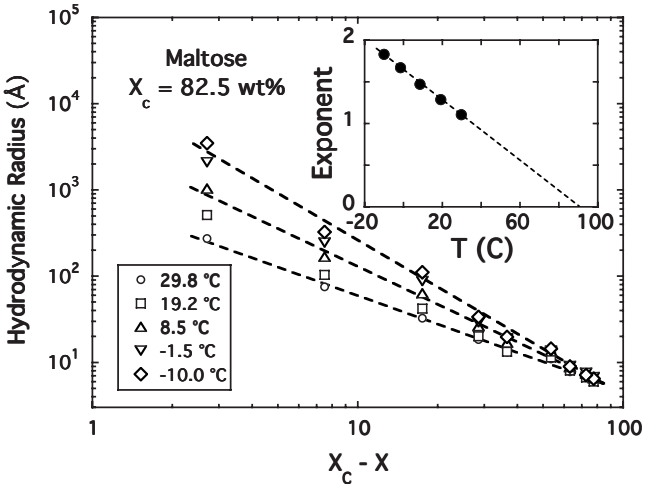

FIG. 8. The hydrodynamic radius of maltose obtained using water as the Brownian medium is plotted against the wt % of maltose relative to the critical wt %, X_c=82.5 for five different temperatures (shown in key). The dashed lines are a fit to Eq. (12) for 29.8, 8.5, and −10 °C. The power law is largely preserved, but the slope (i.e., the power law exponent) increases with decreasing temperature. Inset shows how the power law exponent varies with temperature. The dashed line is a linear extrapolation indicating that the cluster growth vanishes in the vicinity of 90 °C.

$$S(q) = \frac{I(q)}{I(0)} = \frac{1}{1 + q^2\xi^2}, \tag{11}$$

and their size can be estimated from the slope of a plot (see inset to Fig. 6 for one example) of the inverse scattered intensity against q^2. Results of this analysis produced values of ξ that are included in Fig. 6 and are seen to agree well with the values of R_H obtained using water as the Brownian fluid.

Returning now to Fig. 6, we see that the cluster size is increasing with increasing sugar concentration in an accelerating manner with a trajectory that appears to diverge somewhere above 80 wt % sugar. Guided by MD simulations that have suggested the percolation of a hydrogen bonded carbohydrate network, we inquire as to whether the increasing cluster size is consistent with the sort of power law growth arising from self-similar cluster-cluster aggregation found in percolation processes [22]. To test this, we have plotted in Fig. 7 the hydrodynamic radius for maltose at room temperature in the usual double-log manner as a function of concentration relative to some critical percolation threshold concentration, X_c. In the figure, we present the result with a variety of possible choices for X_c between 80 and 90 wt % seeking the value of X_c that best produces a power law over the entire range. We find for maltose that a power law is best obtained for $X_c \approx 82.5(\pm 1)$ wt %. Remarkably, this power law appears to be a *universal* feature of sugar solutions. As illustrated in the inset to Fig. 7, the same power law growth (same exponent and X_c) is observed also for glucose as well as a limited set of data for sucrose [23] at the same fixed temperature. Note also, that although this power law seen for the hydrodynamic radius was determined using water as the Brownian medium, the viscosity of water at 20 °C is a fixed constant and thus the power law is preserved for the drag coefficient (ζ) which itself is independent of our choice for the Brownian medium. The significance of the common critical percolation threshold at X_c=82.5 wt % suggests an additional connection with percolation. In continuum percolation [24], appropriate to an amorphous material, the percolation threshold for three-dimensional (3D) percolation occurs at *volume* fraction of approximately 15–16 vol %. For these sugars, this corresponds to a weight fraction of 89 wt %, not far from what we observe.

The exponent of the power law, however, appears to be temperature dependent. In Fig. 8, we present the hydrodynamic radius of maltose with X_c=82.5 wt % for five different temperatures equally divided across the range of data in Fig. 4. In each instance, X_c=82.5 wt % does well in producing a power law growth of the form

$$R_H = R_M \left(\frac{X_c - X}{X_c} \right)^{-y(T)}, \tag{12}$$

but the slope of the growth decreases with increasing temperature. In the inset to Fig. 8, we have plotted the observed power law exponent, $y(T)$, for maltose and see that it extrapolates to zero at approximately 90 °C, close to the boiling point of water. What is the significance of this result? We believe it is a reflection of the role of hydrogen bonding in the formation of these sugar clusters. In water, the strength of a hydrogen bond is insufficient (relative to kT) to maintain a condensed state at the boiling point. These same hydrogen bonds are responsible for intermolecular binding of sugar molecules and their effectiveness is similarly reduced as the temperature increases. Near 100 °C, they are unable to form stable bonds and, as a result, cluster growth is inhibited. Conversely, with lowering of temperature, the intermolecular bonding is enhanced and in these instances clustering is pro-

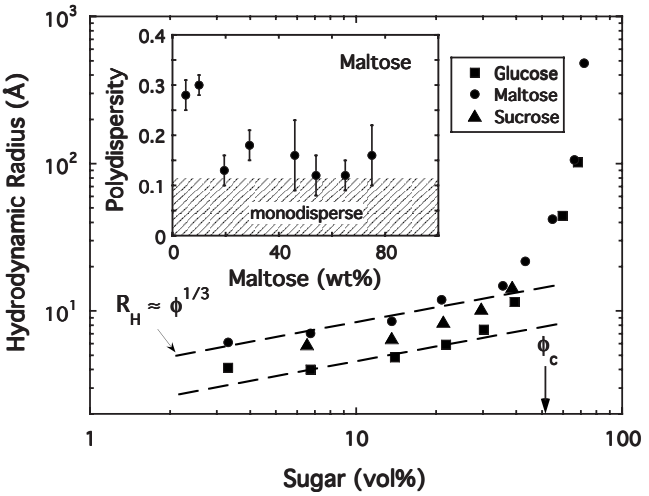

FIG. 9. The hydrodynamic radius of three sugars obtained using water as the Brownian medium are plotted against the vol % of sugar. Below the cluster-cluster aggregation threshold, $\phi_c \approx 50$ vol %, the cluster size is well described (dashed lines) by Eq. (15) for an equilibrium cluster phase. Above this threshold, cluster-cluster aggregation results in accelerated growth. The inset shows how the polydispersity index, defined by Eq. (14) varies with sugar concentration. For all but the very dilute concentrations, the solutions are approximately monodisperse.

moted leading to the more rapid growth rate (power law exponent) that we observe. This observation is consistent with the dielectric study of glucose by Kaminski *et al.* [13], who concluded that glucose clusters become unstable and disintegrate at temperatures in excess of 93 °C.

Power law growth of the mean cluster size is one hallmark of percolation. But, so too is the development of a broad distribution of cluster sizes wrought by the inherent random aggregation of smaller clusters. Although our diffusive relaxation is well described by Eq. (4), we have also performed a cumulant analysis [25] of our autocorrelation functions in order to characterize the level of polydispersity. Briefly, in this analysis the argument of the exponential in Eq. (4) is expanded as a power series of the form

$$\ln(S(q,t)) = \ln A - K_1 t + (K_2/2)t^2 - \cdots, \tag{13}$$

where

$$K_1 = q^2\langle D\rangle,$$

$$K_2 = q^4\langle (D - \langle D\rangle)^2\rangle,$$

and the polydispersity index,

$$p = \frac{K_2}{K_1^2} = \frac{\langle (D - \langle D\rangle)^2\rangle}{\langle D\rangle^2}, \tag{14}$$

provides a normalized measure of the variance in D (or equivalently in R). A value of $p \leq 0.1$ is considered monodisperse and indeed a cumulant analysis performed for the autocorrelation obtained from a nominally monodisperse suspension of polystyrene spheres yielded $p \approx 0.10$. Results for maltose are provided in Fig. 9 where it can be seen that, for concentrations greater than 15 wt %, $p \approx 0.15 \pm 0.03$ and would be characterized as marginally monodisperse. Strong deviations from monodispersity ($p \approx 0.3$) are only seen for the very dilute concentrations and are not altogether unexpected since at these concentrations the clusters contain only a very few monomers.

Thus it would appear that, although the cluster growth leads to the formation of a percolated network near 82.5 wt %, the formation of intermediate clusters is much unlike that seen in such phenomena as percolation, gelation, and diffusion limited aggregation (DLA) where cluster aggregates result from purely random chance that a connection is formed between pre-existing clusters. In both DLA and gelation, cluster formation occurs in a nonequilibrium sense; once the conditions are appropriate for connections to form (i.e., the temperature of a sol is lowered below its gel temperature or the particles of a colloid are rendered unstabilized by chemical alteration of the solution), the cluster growth proceeds, unchecked, forming a broad distribution of clusters until an infinite size is reached. Here, we find instead the formation of equilibrium clusters with a surprisingly monodisperse distribution of sizes that shares greater similarity to recently discussed "cluster phases" found in certain colloidal systems [15]. As described by Sciortino [15], the cluster phase consists of "an equilibrium state in which colloidal particles partition into stable clusters via the competition between attraction (which favors cluster growth at low T) and long-range repulsion (which favors low local particle densities and, therefore, small aggregates)." This competition promotes narrow size distributions and such cluster phases have now been reported by several researchers [14–16].

A prominent feature of the cluster phase is a dependence of the cluster size on volume fraction, ϕ, of the form

$$R \propto A(T)\phi^{1/3}, \tag{15}$$

which is predicted by theory [17] and has been observed recently in colloidal solutions of the protein lyzosyme by Stradner *et al.* [14]. In Fig. 9, we test this prediction by plotting R_H as a function of the volume fraction on a double-logarithmic scale and find that for concentrations less than about 40 vol %, the cluster growth does appear to favor the cluster phase prediction. However, the growth is much more accelerated at higher volume fractions.

We propose that there are, in fact, two stages of cluster growth at work in these sugar solutions. In the cluster phase, sugar clusters grow in relative isolation, essentially accreting sugar molecules until they reach a stable, monodisperse size set by Eq. (15) with a volume on the order of $V_c = 4\pi R^3/3$. These isolated clusters are separated on average by a distance b on the order of

$$b \approx n_c^{-1/3} = (V_c/\phi)^{1/3} \approx (4\pi R^3/3\phi)^{1/3} = (4\pi/3)^{1/3}A(T), \tag{16}$$

which is independent of ϕ.

As ϕ increases, these isolated clusters grow but maintain a nearly monodisperse size distribution. This in turn, allows b to remain fixed and largely independent of the volume fraction. However, at some critical volume fraction when $2R \approx b$, or

$$\phi_c \approx \frac{\pi}{6} \approx 0.5, \tag{17}$$

these isolated clusters must overlap. In Fig. 9, we see that it is near this same critical concentration where the cluster phase growth law [Eq. (15)] starts to falter and a second stage of growth, involving traditional cluster-cluster aggregation begins. This second process is much like percolation with an inherent self-similarity that terminates with the formation of a continuous carbohydrate network formed near $X_c = 82.5$ wt %.

Overall, we find that these sugars appear predisposed to cluster formation at all levels of concentration including those dilute levels for which vitrification would be challenging. Given this proclivity, it seems likely that most any protein that interacts by hydrogen bonding would only aid in the clustering process by serving as a nucleation site for sugars to begin clustering. We thus conclude that the findings of the present work are more supportive of the water replacement model for cryopreservation. In future work, we plan to introduce proteins into these solutions and use fluorescence correlation spectroscopy as a selective probe of protein dynamics to determine whether sugars do indeed preferentially accrete to the protein.

V. CONCLUSION

Our dynamic light scattering study reveals a universal power law growth of sugar clusters in aqueous solutions of glucose, maltose, and sucrose as a function of sugar concentration. In all three sugars there appears to be a divergence of the cluster size transpiring at a critical percolation threshold near 83 wt % sugar that may be linked to percolation in the classical continuum percolation model. However, this aggregation process appears to be preceeded (at low concentrations) by the formation of a cluster phase consisting of a colloid of equilibrium-sized, nearly monodisperse, clusters stablilized by a long-range repulsive interaction.

ACKNOWLEDGMENTS

This work was supported by Award No. R01EB009644 from the National Institute Of Biomedical Imaging And Bioengineering.

[1] B. Han and J. C. Bischof, Cell Preservation Technology **2**, 91 (2004).
[2] K. B. Storey and J. M. Storey, Annu. Rev. Ecol. Syst. **27**, 365 (1996).
[3] J. H. Crowe, J. F. Carpenter, and L. M. Crowe, Annu. Rev. Physiol. **60**, 73 (1998).
[4] F. Franks, Pure Appl. Chem. **65**, 2527 (1993).
[5] J. L. Green and C. A. Angell, J. Phys. Chem. **93**, 713 (1989).
[6] J. H. Crowe, L. M. Crowe, and D. Chapman, Science **223**, 701 (1984).
[7] E. R. Caffarena and J. R. Grigera, Carbohydr. Res. **300**, 51 (1997); **315**, 63 (1999).
[8] C. J. Roberts and P. G. Debenedetti, J. Phys. Chem. B **103**, 7308 (1999).
[9] N. C. Ekdawi-Sever, P. B. Conrad, and J. J. de Pablo, J. Phys. Chem. A **105**, 734 (2001).
[10] S. L. Lee, P. G. Debenedetti, and J. R. Errington, J. Chem. Phys. **122**, 204511 (2005).
[11] A. Lerbret, P. Bordat, F. Affouard, M. Descamps, and F. Migliardo, J. Phys. Chem. B **109**, 11046 (2005).
[12] D. L. Sidebottom, Phys. Rev. E **76**, 011505 (2007).
[13] K. Kaminski, E. Kaminska, K. Adrjanowicz, Z. Wojnarowska, P. Wlodarczyk, K. Grzybowska, M. Dulski, R. Wrzalik, and M. Paluch, Phys. Chem. Chem. Phys. **12**, 723 (2010).
[14] A. Stradner, H. Sedgwick, F. Cardinaux, W. C. K. Poon, S. U. Egelhaaf, and P. Schurtenberger, Nature (London) **432**, 492 (2004).
[15] F. Sciortino, S. Mossa, E. Zaccarelli, and P. Tartaglia, Phys. Rev. Lett. **93**, 055701 (2004).
[16] S. Guillot, M. Delsanti, S. Desert, and D. Langevin, Langmuir **19**, 230 (2003).
[17] J. Groenewold and W. K. Kegel, J. Phys. Chem. B **105**, 11702 (2001).
[18] B. J. Berne and R. Pecora, *Dynamic Light Scattering* (Wiley, New York, 1976).
[19] A.V. Wolf, M. G. Brown, and P. G. Prentiss, in *Handbook of Chemistry and Physics*, 64th ed. (CRC Press, Boca Raton, Florida, 1985).
[20] M. Rampp, C. Buttersack, and H.-D. Ludemann, Carbohydr. Res. **328**, 561 (2000).
[21] F. Ould-Kaddour and D. Levesque, Phys. Rev. E **63**, 011205 (2000).
[22] D. Stauffer, *Introduction to Percolation Theory* (Taylor & Francis, Philadelphia, 1985).
[23] The radius of sucrose appears intermediate between that of glucose and maltose. This is thought to be a consequence of the enhanced intramolecular hydrogen bonding present in sucrose (see Ref. [11]) that promotes a folded molecular structure.
[24] H. Scher and R. Zallen, J. Chem. Phys. **53**, 3759 (1970); R. Zallen, *The Physics of Amorphous Solids* (Wiley, New York, 1983).
[25] D. E. Koppel, J. Chem. Phys. **57**, 4814 (1972).